Separation and Purification Technology, Volume 66, Issue 3, 7 May 2009, Pages 578-585

Accepted Manuscript

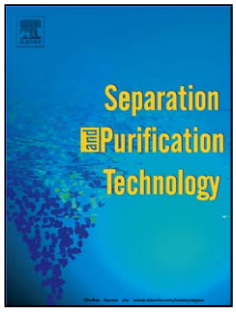

Title: Synthesis and characterisation of size-selective nanoporous polymeric adsorbents for blood purification

Authors: D.J. Malik, C. Webb, R.G. Holdich, J.J. Ramsden, G.L. Warwick, I. Roche, D.J. Williams, A.W. Trochimczuk, J.A. Dale, N.A. Hoenich

PII: S1383-5866(09)00031-8
DOI: doi:10.1016/j.seppur.2009.01.016
Reference: SEPPUR 9463

To appear in: *Separation and Purification Technology*

Received date: 14-5-2008
Revised date: 15-1-2009
Accepted date: 26-1-2009

Please cite this article as: D.J. Malik, C. Webb, R.G. Holdich, J.J. Ramsden, G.L. Warwick, I. Roche, D.J. Williams, A.W. Trochimczuk, J.A. Dale, N.A. Hoenich, Synthesis and characterisation of size-selective nanoporous polymeric adsorbents for blood purification, *Separation and Purification Technology* (2008), doi:10.1016/j.seppur.2009.01.016

Synthesis and characterisation of size-selective nanoporous polymeric adsorbents for blood purification

Malik DJ[a]*, Webb C[a], Holdich RG[a], Ramsden JJ[b], Warwick GL[c], Roche I[a], Williams DJ[d],Trochimczuk AW[e], Dale JA[f] and Hoenich NA[g].

[a] Chemical Engineering Department, Loughborough University, Loughborough, Leicestershire, LE11 3TU, United Kingdom.

[b] Department of Materials, Cranfield University, Bedfordshire, MK43 0AL, United Kingdom.

[c] John Walls Renal Unit, Leicester General Hospital, University Hospitals of Leicester NHS Trust, Gwendolen Road, Leicester LE5 4PW, United Kingdom.

[d] Wolfson School of Mechanical and Manufacturing Engineering, Loughborough University, Loughborough, LE11 3TU, United Kingdom

[e] Faculty of Chemistry, Wrocław University of Technology, Wybrzeze Wyspiańskiego 27, 50-370 Wrocław, Poland.

[f] Global Research Centre, Purolite International Limited, Unit D, Llantrisant Business Park, Llantrisant Wales, CF72 8LF, United Kingdom.

[g] Department of Nephrology, University of Newcastle-upon-Tyne, The Medical School, NE2 4HH, United Kingdom.

Abstract

Crosslinked polystyrene codivinylbenzene adsorbent microspheres with median diameters between 40 and 300 micrometres, with an enhanced proportion of mesopores in the range 4-10 nm, have been synthesised using a membrane emulsification technique. The aim was to develop an adsorbent for the selective removal of middle molecular weight uraemic toxins (size range 0.5 – 20 kDa), e.g. β_2-microglobulin (11.8 kDa), whilst size-excluding larger blood proteins e.g. serum albumin (MW 69 kDa). Using inverse size exclusion chromatography, the role of size exclusion has been demonstrated using hen egg

* To whom correspondence should be addressed. Tel. +44 1509 222507; Fax: +44 1509 223923; email: d.j.malik@lboro.ac.uk,

lysozyme (a surrogate for β_2-microglobulin) and human serum albumin as model proteins for batch adsorption studies. The adsorbent sample possessing a nanoporous structure with pores predominantly smaller than 10 nm successfully size-excludes serum albumin whilst displaying significant adsorption capacity for the middle molecular weight lysozyme (14.3 kDa).

Keywords: Middle molecular weight toxins; haemoadsorption; inverse size exclusion chromatography; haemodialysis; microspheres; membrane emulsification

1. Introduction

Worldwide, around 1.8 million people are undergoing treatment for end-stage renal disease (ESRD) [1], of which around 1.4 million (~77%) are on dialysis treatment (89% of which are on haemodialysis and 11% on peritoneal dialysis) and the rest (23%) are living with a functioning renal transplant. Haemodialysis membranes are permeable to low molecular weight solutes, however, the removal of potent middle molecular weight uraemic toxins by this method is quite incomplete [2]. While the identity of many of these toxins remains unknown, elevated blood concentrations of certain middle molecular weight proteins (MMW ~ 10 kDa – 20 kDa) such as β_2-microglobulin (β_2M, MW 11.8 kDa) have been associated with amyloid deposition [3] and inflammatory cytokines (e.g. IL-1β, MW ~18 kDa) have been associated with an elevated level of immune system activity [4]. These are important target molecules for extracorporeal removal. In established renal failure, many other molecules in the MMW range accumulate [5].

An alternative to haemodialysis is to bring the blood extracorporeally in contact with a biocompatible adsorbent. There is increasing interest in the development of adsorption-based systems for the non selective removal of toxins from blood for the treatment of uraemia [6], sepsis [7] and drug overdose [8]. A commercially available polymeric

adsorbent (Lixelle, Kaneka, Japan) designed for the removal of β_2M is being used in Japan for the purification of haemodialysis patients' blood. The adsorbent beads are porous cellulose, modified with hexadecyl groups that adsorb β_2M by nonspecific hydrophobic interactions. Patients treated with the Lixelle column have been shown to have significantly lower levels of β_2M (60–70% reduction compared with initial levels after a 4–5 h treatment session) and concomitantly improved symptoms, including a better ability to undertake daily activities, reduced joint stiffness and pain, as well as a reduction of the appearance of bone cysts [9]. The Lixelle adsorbent capacity is reported to be around 1 mg β_2M per cm^3 of adsorbent [10]. During a 4–5 h haemoperfusion treatment session, a 350 cm^3 column removed 210 mg of β_2M [10] (the typical serum concentration of β_2M in renal patients is around 35 mg l^{-1}). The Lixelle column has also been shown to nonspecifically remove middle molecular weight plasma cytokines (IL-1β, IL-6, IL-8 and TNF-α) in humans with sepsis [11]. At the present time, this treatment is only undertaken in Japan and its (high) cost may exceed the value of the clinical benefits. Other researchers have investigated the use of immobilized antibody-functionalized adsorbents for the selective removal of β_2-M [12]. Reported adsorption capacity (0.4 mg β_2M cm^{-3} adsorbent) was comparable with the Lixelle adsorption data, but this approach is even more expensive.

There is therefore a strong motivation to develop new, less costly polymeric adsorbents possessing suitable physicochemical attributes that may prove clinically beneficial. We wondered whether such attributes might be achieved relatively simply by tailoring the mesoporous structure (4–10 nm range) using conventional suspension polymerization synthesis techniques. Ideally the external bead surface should have low affinity for all proteins;for example, by employing an ultrahydrophilic external surface coating for the adsorbent bead (see Figure 1); and may require surface modification to reduce adverse

interactions with blood that may lead to platelet activation, etc., -- proteins adsorbing on hydrophobic surfaces are likely to be permanently denatured [13] and recognised as foreign by the immune system. The walls of the internal pores should have high affinity for all proteins (e.g., but could through nonspecific hydrophobic interactions). Suitable polymeric adsorbents must furthermore fulfil a number of clinical requirements: inter alia, during haemodialysis, the amount of heparinized blood in the extracorporeal circuit (whose volume is typically 250–300 cm^3) and the time a portion of blood spends in the extracorporeal circuit is necessarily limited (typical blood flow rate during haemodialysis is 250–400 $cm^3\ min^{-1}$) to prevent blood coagulation and minimize platelet activation. In terms of an efficient blood purification column, these requirements translate into the following design criteria: (i) small column size, implying a high adsorption capacity per unit volume; (ii) fast adsorption kinetics, (implying a small bead size with a short diffusion path length); (iii) low pressure drop across the column, (implying a short bed length) and preferably monosized beads to avoid low bed porosity.

Physiologically essential blood proteins such as serum albumin (HSA, MW 69 kDa) are present at a very high concentration (HSA 40 g l^{-1} compared with β_2M ~ 35 mg l^{-1}), and ideally they should not be removed during haemoperfusion. Moreover, if adsorption were nonspecific, the high concentration (3 orders of magnitude higher than β_2M!) of HSA would flood the adsorbent surface with HSA and lead to very inefficient removal of the uraemic toxins (14). Bearing in mind that ideally the adsorbent should remove a range of middle molecular weight molecules (i.e., smaller than albumin and other abundant blood proteins such as immunoglobulin and fibronectin), selectivity for the toxins in the presence of competing solutes may conveniently be achieved by size exclusion (Figure 1); the hydrodynamic diameter of HSA is ~7 nm and of MMW toxins such as β_2M ~4 nm. Note

that size exclusion is routinely employed for the analytical determination of polymer molecular weights (size exclusion chromatography, SEC).

Control of pore structure in crosslinked polymeric resins has been investigated widely in the literature [15-30], with the conclusion that controlling the maximum pore size in an adsorbent bead requires judicious selection of the diluents used as porogens; and the crosslinking degree and to a lesser extent polymerization temperature and initiator (type and concentration) influence the pore structure within the polymer adsorbent bead.

Since the adsorption process requires the toxin to diffuse within the adsorbent bead (where most of the surface for adsorption is present), the kinetics of the process will be limited by intrabead mass transfer and hence depend on the size of the adsorbent beads. There are two conflicting factors at play here, (i) whilst a small bead size will result in faster toxin removal kinetics (desirable), the price to be paid will be (ii) a high external surface area per unit volume of packed-bed, which may result in adverse blood-surface interactions and certainly a higher pressure drop across the adsorbent packed-bed. This is undesirable since shear damage to blood (leading to haemolysis) is clinically dangerous.

The aim of the work presented here was to develop an adsorbent material that would successfully size-exclude serum albumin while allowing middle molecular weight proteins access to the internal surface of the adsorbent. We have focused on copolymers of styrene divinylbenzene, PSDVB, because they are known to be good hydrophobic adsorbents.

2. Experimental Materials and Methods

2.1. Adsorbent Preparation

During the suspension polymerization process, a mixture of styrene and divinylbenzene (oil phase) was dispersed in an aqueous solution (the continuous phase) using a novel membrane emulsification process (described below). The reaction was initiated using benzoyl peroxide as the initiator (1% of the monomer concentration by weight). Porogens studied included toluene and mixtures of toluene with precipitating media such as undecane and naphthalene. The exact compositions of the monomer phase can be seen in Table 1. The monomer to porogen ratio was kept at 1:1 by weight. The nomenclature used to label the adsorbents is explained by the following example: PSDVB3:5TolNap5:2 (from Table 1) was prepared by mixing equal amounts (w/w) of a mixture containing styrene and DVB (ratio 3:5) with a porogen mixture of toluene and naphthalene (ratio 5:2).

The emulsion droplets were stirred throughout the reaction period and stabilized using poly(vinyl alcohol) (PVA) to keep the droplets from coalescing during the “sticky” phase. Once the polymerization reaction was complete, the polymer beads were separated from the continuous phase by filtration.

2.2. Membrane emulsification

A conventional stirred tank system for generating an O/W (oil in water) emulsion results in a heterogeneous population of droplet sizes due to the nonuniformity of the shear field. Hence a membrane emulsification process was investigated (Figure 2). By using a controlled pore size membrane (supplied by Micropore Technologies (UK) Ltd) a much narrower size distribution than via the conventional method can be produced. For the production of beads with a mean size of 40 μm, a circular 10 μm pore membrane was used. The monomer mixture was injected through the membrane into the aqueous solution using a syringe pump at an injection rate of 0.4 cm^3 min^{-1}. The droplets were sheared off

the membrane surface using a paddle stirrer. The continuous phase used to stabilize the oil droplets was a solution of 3% w/w PVA (Mowiol™ 40-88) and 3.3% w/w NaCl. The droplet size was controlled by shear at the membrane surface (influenced by the viscosity of the continuous phase and by the stirrer speed) and membrane pore size.

The droplets formed in the dispersion cell were then transferred to a reaction vessel containing an aqueous solution of 4.5% PVA and 3.3% NaCl. The polymerization reaction was carried out at 80 °C for 24 h. Adsorbent beads were subsequently separated using a Buchner funnel and Whatman GF/B glass fibre filters, washed with hot distilled water to remove the PVA and NaCl and rinsed with acetone to remove any residual water, and soxhlet extracted for 8 h with toluene to remove any unreacted monomers. Finally, the adsorbent beads were dried under vacuum at ambient temperature overnight. Bead sizes were evaluated using a Coulter LS130 instrument. The amount of material produced per batch was typically ~50 cm^3 of beads compared with ~100 cm^3 from a conventional stirred tank system.

2.3. Inverse Size Exclusion Chromatography

Size exclusion chromatography [31-33] is conventionally used to size-separate solutes, e.g. proteins [34, 35] that . It is routinely used for the determination of the molecular weight distribution of polymer samples [36]. Inverse size exclusion chromatography (ISEC) may be used to investigate the pore structure of a swollen polymer adsorbent [37-41]. The technique employs a number of probe molecules (normally polymers of narrow molecular weight distribution) that do not interact with the surface of the adsorbent material. The retention time of each probe within a packed column of the adsorbent material reflects the degree to which the probe is prevented from accessing the pore volume of the adsorbent

beads (and consequently the adsorbent bed). This can be expressed as the exclusion coefficient, K_d, which is defined as:

$$K_d = \frac{V_R - V_0}{V_T - V_0} \quad (1)$$

where V_R is the solute elution volume, V_0 is the interparticle void volume and V_T is the total mobile phase volume. A probe molecule too large to enter the adsorbent beads allows the characterization of the interparticle void volume (V_0), and by using a molecule small enough to enter all the pores, total accessible mobile phase volume (V_T) is quantified. Thus for each calibration probe of intermediate size, the corresponding K_d may be determined. The retention volumes and retention times are related by the flow rate of the mobile phase, i.e.

$$K_d = \frac{t_R - t_0}{t_T - t_0} \quad (2)$$

where t_R is the solute retention time, t_0 is the retention time of the excluded probe and t_T is the retention time of the probe that can access the whole pore volume. Thus, values for K_d range from 0 (completely excluded probe) to 1 (probe that can access the whole pore structure), and $1 - K_d$ gives the fraction of the pore volume inaccessible to a particular probe molecule.

For analysis of the PSDVB the mobile phase was tetrahydrofuran (THF), and the probe molecules were various low polydispersity calibration polystyrenes and toluene (the smallest). Table 2 shows the relationship between polymer probe molecular weight and the solute viscosity radius R_η (in cm) is given by the relation:

$$R_\eta = \left(\frac{3[\eta]M}{10\pi N_A} \right)^{\frac{1}{3}} \qquad (3)$$

where N_A is Avogadro's number, M is the solute molecular weight and [η] is the intrinsic viscosity ($cm^3\ g^{-1}$) [37]. R_η accounts for both the solute mass and shape (which are also reflected in the intrinsic viscosity) and thus is used as a universal calibration parameter for SEC.

Adsorbents with modal bead sizes of 30–40 μm were swollen in THF for 24 h before being slurry-packed under pressure (250 bar) into stainless steel columns 4.6 mm in diameter and 25 cm long. After packing, THF was passed through the columns overnight at a flow rate of 0.1 $cm^3\ min^{-1}$ to ensure the bed was settled and any impurities removed. The conditions for the analysis were: column temperature 35 °C, THF flow rate 0.5 $cm^3\ min^{-1}$ (Kontron Instruments HPLC pump 420), and 100 μl of 1.5 g l^{-1} polystyrene standard solution were injected. Detection of the standards was with a Perkin Elmer u.v./vis. Lambda 2 spectrometer fitted with a flow cell operating at a wavelength of 254 nm. Retention times for each standard were compiled and values for K_d calculated according to eqn (2).

2.4. Porosity/Pore Size Distributions

The pore size distributions of the various adsorbents produced were analysed in the dry state using nitrogen adsorption (77 K) on a Micromeritics ASAP 2000 instrument. Additionally, data for Amberlite XAD4 (Rohm & Haas), a commercially available and widely studied styrene co-divinylbenzene mesoporous adsorbent, is also reported as an example of a widely used adsorbent. All of the adsorbents were dried overnight from toluene under

vacuum at ambient temperature. The nitrogen isotherm was fitted with the BET model to evaluate the surface area, and total pore volume was also recorded. Incremental and cumulative pore size distributions were evaluated from the nitrogen adsorption isotherm data using mean-field density functional theory (DFT) [42].

2.5. Albumin and lysozyme uptake

The prohibitively high cost of β_2-M for the physicochemical characterization experiments led us to seek a low-cost protein of similar size to β_2-M, and readily available in a pure state. Lysozyme (hen egg white, MW 14.4 kDa, size ~ 4 nm) was used as a surrogate for β_2-M (MW 11.8 kDa, size ~ 4 nm). The purpose of the single solute *in vitro* adsorption studies was to demonstrate the accessibility of the adsorbent internal surface to solutes of size ~ 4 nm and concomitant rejection of the significantly larger HSA (and a fortiori the even larger immunoglobulins).

Characterising adsorbents in terms of adsorption capacity and adsorption kinetics is possible experimentally using a batch stirred tank reactor. The time to equilibrate/saturate the adsorbent with protein diffusing from the bulk solution to the interior of the adsorbent particle depends on the particle size of the adsorbent beads and the effective diffusivity of the protein in the interior of the adsorbent. A small number of experiments under carefully controlled conditions was undertaken.

The dynamic batch adsorption experiments were conducted in a thermostated (37 °C) 0.5 l stirred tank reactor fitted with an overhead agitator and baffles. Influence of stirrer agitation rate on the kinetics of the adsorption process was investigated and the stirrer agitation speed was selected such that external mixing effects no longer influenced the kinetics of the adsorption process (Biot number $Bi = k_f R_p / D_e > 100$, where k_f is the external film mass

transfer coefficient, R_p the bead radius and D_e the solute effective diffusivity in the adsorbent pores). 0.5 l of pH-buffered (containing HEPES at a concentration of 10 mM, NaCl 100 mM, pH 7.2) protein solution (containing either lysozyme at an initial concentration of 100 mg l^{-1} or human serum albumin at an initial concentration of 200 mg l^{-1}) was brought into contact with a known amount of preswollen adsorbent, XAD4 or PSDVB3:5TolNap5:2. Solution samples were taken at regular intervals until no change in solution protein concentration was recorded. The solution protein concentration was measured using reverse phase HPLC (Agilent 1100 series) equipped with a diode array detector (detection wavelength λ = 230 and 290 nm for albumin and lysozyme, respectively) and a C18 analytical column (Supelco, UK). The mobile phases were A: ultrapure water with 0.5% trifluoroacetic acid (TFA) and B: acetonitrile with 0.1% TFA. A linear gradient was used starting at (98% A : 2% B) and ending at (20% A: 80% B) over 60 minutes followed by a step change back to (98% A : 2% B) for 10 minutes to equilibrate the column for the next sample. The combined mobile phase flow rate was set at 1 cm^3 min^{-1}, the column temperature was set at 40 °C and the sample injection volume used was 100 μl. The reported adsorption capacity values (q*, mg g^{-1}) correspond to saturation protein uptake values whereas the fractional uptake F(t) = q(t)/q* represents the normalised uptake at a given time point (t).

3. Results and Discussion

3.1. Bead Size Control

Figure 3 shows representative bead size distributions for two of the materials generated using the membrane emulsification technique. The data illustrate the effect of shear at the membrane surface on the droplet size distribution. Median diameters within the range of 30 to 300 μm could be controllably produced. Table 3 summarizes the bead size

information for the three adsorbents studied using the inverse size exclusion chromatography (ISEC) technique.

Adsorbents used in fixed-bed haemoperfusion systems tend to have bead sizes larger than 300 μm. The ISEC work required the bead size to be an order of magnitude smaller (to aid resolution of the different probe retention peaks). Thus, the effect of the smaller bead size on the resulting pore size distribution was evaluated. Nitrogen adsorption/desorption data was obtained for two PSDVB3:5TolUn1:0 samples with median bead sizes of 37 and 120 μm respectively. It is evident from Figure 4 that the pore structure is essentially invariant for polymerization within oil droplets of different sizes over this range. Thus, we can infer that ISEC measurements on material of smaller average size may be used to provide insight into the pore structure of larger beads prepared under similar suspension polymerization conditions.

3.2. Control of pore structure

The three monomer and porogen combinations investigated in the present study focus on the use of toluene, a good solvent for polystyrene, to generate small pores, thereby reducing the maximum pore size. Figure 5 shows the normalized incremental pore volume distributions for the materials studied. Table 4 provides a summary of the BET surface area, total pore volume and discretized surface area and pore volumes for pores in the ranges 2–10 nm and 10–50 nm.

Comparing the pore structure of the adsorbent sample prepared using undecane (PSDVB1:1TolUn9:1) with XAD4 shows that while having different overall surface areas and pore volumes (Table 4), the two samples have similar pore size distributions (Figure 5), especially in the region above 10 nm. PSDVB3:5TolUn1:0 and PSDVB3:5TolNap5:2

both have similar cut-offs at ~20 nm; however, PSDVB3:5TolNap5:2 has a smaller fraction of its pores in the region above 10 nm, which was the desired synthesis objective for promoting serum albumin exclusion.

Analysis of the adsorbent materials in the swollen state was done using ISEC themain drawback of which is the requirement that the mobile phase be THF (to minimize nonspecific interactions between polystyrene probes and the adsorbent), a good solvent for polystyrene. This may result in polymer segment swelling with the undesirable effect of changing the internal pore structure compared with that of the polymer when suspended in water or in contact with blood. There is however evidence that low-temperature vacuum drying of a crosslinked polymeric adsorbent (medium to high crosslinking density) from a solvent (either a poor or a good one) followed by nitrogen porosimetry may allow the porous structure in that solvent to be retained and hence recorded [21]. Thus, if the maximum pore size (pore cut-off) of the methanol-dried adsorbent (methanol is a poor solvent for polystyrene) is the same as that for a toluene-dried sample, then it is reasonable to assume that the results from the ISEC technique may be used to predict the molecular weight cut-off for the adsorbent samples in THF. The adsorbents prepared in this study have a high crosslinking degree and would be expected to have a stable pore structure in any case. Figure 6 shows the cumulative pore volume distributions of PSDVB3:5TolNap5:2 when dried from toluene, acetone and methanol respectively. Figure 6 clearly shows that there are differences in the pore volumes for this material when swollen in different solvents. The normalized data would highlight any differences in the distribution of pores due to swelling in different solvents. As the normalized distributions overlay on one another, this suggests that while the total pore volume changes, the distribution of the pores (greater than ~1 nm) and the pore cut-off remains unchanged. Hence we may use ISEC with confidence.

3.3. ISEC

Eight polystyrene standards in THF were used to probe the three adsorbents under investigation. XAD4 was not evaluated using ISEC as commercial material is not available in the appropriate bead size range (less than 50μm); PSDVB1:1TolUn9:1 with its comparative pore structure was used as a surrogate for XAD4. 8 probe standards and toluene (see Table 2) were individually injected into the column packed with the adsorbent material and a composite chromatogram overlaying all the peaks for each sample was generated (see Figure 7). From these chromatograms, the exclusion coefficients K_d were calculated (eqns (1) and (2)). K_d represents the fraction of the pore volume which the probe is able to access and this has been plotted in Figure 8 for the PSDVB1:1TolUn9:1 and PSDVB3:5TolNap5:2 polymer samples.

Serum albumin has a nominal size of ~7 nm (hydrodynamic radius ~ 3.5 nm). Reference to data in Table 2 shows that this falls between polystyrene probe standards PS 10 kDa, R_η 2.8 nm and PS 20 kDa, R_η 4.7 nm. The chromatogram for PSDVB1:1TolUn9:1 (Figure 7A) clearly shows that the 20 kDa polystyrene probe (peak 7) is able to enter some part of the adsorbent pore structure. The chromatogram for PSDVB3:5TolNap5:2 shows the peak for the 20 kDa polystyrene standard bunched up with the peak for the 1 MDa polystyrene standard, implying rejection of the probe from the adsorbent. Resolution of probes below 10 kDa is possible with the adsorbent material packed in this column. Figure 8 shows the fraction of the pore volume accessible to albumin-sized probes. Thus, on the basis of the ISEC data, the adsorbent material PSDVB3:5TolNap5:2 possesses a well defined mesopore structure (< 10 nm) capable of size-excluding serum albumin whilst allowing middle molecular weight solutes access to the internal surface of the adsorbent.

3.4. Albumin and lysozyme uptake

Analysis of protein equilibrium uptake data

The protein adsorption data obtained for XAD4 and PSDVB3:5TolNap5:2 are presented in Table 5. The saturation capacity values (q*) for lysozyme (LYZ) were 59 mg g^{-1} for PSDVB3:5TolNap5:2 and 330 mg g^{-1} for XAD4. The saturation capacity values (q*) for human serum albumin (HSA) were 2.2 mg g^{-1} for PSDVB3:5TolNap5:2 and 95 mg g^{-1} for XAD4. The adsorption capacity values were found to be concentration-independent (irreversible adsorption). This is fairly common for single protein adsorption studies, where surface coverage has been found in many cases to equate to quasi-monolayer adsorption [43, 44]. The protein saturation capacity values were found to correlate with the surface area accessible to lysozyme (22 m^2 g^{-1}) and albumin (0.9 m^2 g^{-1}) for PSDVB3:5TolNap5:2 (nitrogen porosimetry data) determined on the basis of size exclusion from pores smaller than 6 nm for lysozyme and 14 nm from albumin. This corresponds to surface coverage Γ of 2.7 mg m^{-2} for lysozyme and 2.4 mg m^{-2} for albumin. Analysis of protein saturation data for XAD4 using a similar basis as for PSDVB3:5TolNap5:2 yields the surface areas accessible to lysozyme (120 m^2 g^{-1}) and albumin (40 m^2 g^{-1}). This corresponds to Γ = 2.8 mg m^{-2} for lysozyme and 2.4 mg m^{-2} for albumin. These values are comparable to jammed, randomly adsorbed monolayer coverages reported previously [45, 46].

Batch adsorption dynamics

In addition to evaluation of the protein saturation uptake, time series data were modelled using the irreversible adsorption model proposed by Suzuki and Kawazoe [47] to extract solute intraparticle diffusivities (D_e). The adsorbent samples used were sieved to obtain tight particle size fractions. Experiments were performed using a single dissolved protein in 0.1M Hepes buffer solution. A summary of the values of the experimental variables used for the batch adsorption experiments are provided in Table 6. The stirrer speed was set to

726 rpm as this was found to minimise external film mass transfer resistance to solute diffusion permitting evaluation of the intraparticle diffusional resistance to mass transfer.

The 1st order differential equation derived by Suzuki et. al. [47] relating the change in solute concentration in the tank to uptake by the adsorbent was solved using Matlab software (version 7). The best fit value of the effective solute diffusivity D_e was found by minimising the sum of the squares of the errors (difference between the model prediction and the experimental data). The best fit intraparticle diffusivity values D_e evaluated for LYZ and HSA adsorption by PSDVB3:5TolNap5:2 and XAD 4 are presented in Table 6. Experimental kinetic data plotted as fractional uptake F(t) curves are presented in Figure 9; the model predictions are shown as solid curves.

The fitted intraparticle diffusivity values D_e obtained for the lysozyme adsorption data suggested that the uptake kinetics for PSDVB3:5TolNap5:2 ($D_e = 4 \times 10^{-13}$ m^2 s^{-1}) are in order of magnitude slower in comparison with XAD4 ($D_e = 4 \times 10^{-12}$ m^2 s^{-1}). The data in Figure 9 shows slower lysozyme uptake by XAD4 due to the larger particles size for XAD4 (d_p = 576 μm) compared with PSDVB3:5TolNap5:2 (d_p = 28 μm). The slower adsorption kinetics may be attributed to the tighter mesopore structure within PSDVB3:5TolNap5:2, manifested in a reduction in the magnitude of the effective diffusivity of the solute within the adsorbent particle.

HSA ($D_e = 5 \times 10^{-11}$ m^2 s^{-1}) adsorption kinetics for XAD4 was found to be faster in comparison with lysozyme ($D_e = 4 \times 10^{-12}$ m^2 s^{-1}) removal. HSA is able to access only a fraction of the adsorbent pore structure, which appears to provide little hindrance to the diffusion of the solute. The effective diffusivity is similar in magnitude to the free solution diffusivity for HSA (6.1 x 10-11 m^2 s^{-1}). PSDVB3:5TolNap5:2 adsorption capacity for HSA

was small suggesting predominantly adsorption on the external bead surface. The fitted intraparticle diffusivity was similar in magnitude to the free solution diffusivity for HSA (6.1 x 10-11 m^2 s^{-1}).

4. Conclusions

Controlling the internal pore structure of poly(styrene-divinylbenzene) adsorbents (pore size less than 10 nm) is a route to enabling the removal of middle molecular weight proteins whilst excluding larger molecules like serum albumin. A styrene-containing adsorbent (PSDVB3:5TolNap5:2) has been engineered using a membrane emulsification technique and it has been demonstrated that microspheres with median bead diameters in the range of 30 to 300 μm can be prepared by the process. The microspheres have been shown to size-exclude serum albumin whilst allowing removal of smaller proteins (lysozyme, a surrogate for middle molecular weight uraemic toxins). The use of ISEC to probe the pore structure of synthesized adsorbents has proved useful in demonstrating the influence of pore structure control on the size rejection behaviour. The adsorption data provides evidence of the albumin size exclusion phenomena and is currently being investigated in more detail. Preliminary dynamic adsorption studies suggest hindered transport of middle molecules due to the narrow pore size distribution needed to size-exclude human serum albumin.

The kidney is of course an amazingly complex organ [48], and a size-selective adsorbent can of course only provide a very partial replacement of its function, but in the case of renal failure the clinical options are limited, and an improvement in the current poor removal of uraemic toxins by haemodialysis would be of great value for public health. The work reported here is a step in this direction.

Acknowledgements

The authors would like to acknowledge the support of the Engineering and Physical Sciences Research Council (grant nos. EP/C517660/1 and EP/D033837/1).

References

[1] A. Grassman, S. Gioberge, S. Moeller, G. Brown. ESRD patients in 2004: global overview of patient numbers, treatment and modalities and associated trends, Nephrology Dialysis Transplantation 20 (2005) 2587-2593.

[2] H. D. Humes, W. H. Fissell, K. Tiranathanagul. The future of hemodialysis membranes, Kidney International 69 (2006) 1115-1119.

[3] L. M. Dember, B. L. Jaber. Dialysis-related amyloidosis: late finding or hidden epidemic? Seminars in dialysis 19 (2006) 105-109.

[4] J. F. Winchester, J. Salsberg, E. Yoshua. Removal of middle molecules with sorbents, Artificial Cells Blood Substitutes and Immobilisation Technology 30 (2002) 547-554.

[5] R. Vanholder, E. Schepers, N. Meert, N. Lameire. What is uremia? Retention versus oxidation, Blood Purification 24 (2006) 33-38.

[6] J. F. Winchester, P. F. Audia. Extracorporeal strategies for the removal of middle molecules, Seminars in Dialysis 19 (2006) 110-114.

[7] J. F. Winchester, J. Kellum, C. Ronco, J. A. Brady, P. J. Quartararo, J. A. Salsberg, N. W. Levin. Sorbents in acute renal failure and the systemic inflammatory response syndrome, Blood Purification 21 (2003) 79-84.

[8] D. A. Feinfeld, J. W. Rosenberg, J. F. Winchester. Three controversial issues in extracorporeal toxin removal, Seminars in Dialysis 19 (2006) 358-362.

[9] F. Geyjo, Y. Kawaguchi, S. Hara, R. Nakazawa, N. Azuma, H. Ogawa, Y. Koda, M. Suzuki, H. Kaneda, H. Kishimoto, M. Oda, K. Ei, R. Miyazaki, H. Maruyama, M. Arakawa, M. Hara. Arresting dialysis related amyloidosis: A prospective multicentre controlled trial of direct hemoperfusion with a beta(2)-microglobulin adsorption column, Aritifical Organs 28 (2004) 371-380.

[10] H. Kutsuki. Beta(2)-microglobulin-selective direct hemoperfusion column for the treatment of dialysis-related amyloidosis, Biochemica et Biophysica Acta-proteins and Proteomics 1753 (2005) 141-145.

[11] K. Tsuchida, R. Yoshimura, T. Nakatani, Y. Takemoto. Blood purification for critical illness: Cytokines adsorption therapy, Therapeutic Apheresis and Dialysis 10 (2006) 25-31.

[12] E. A. Grovender, B. Kellogg, J. Singh, D. Blom, H. Ploegh, K. D. Wittrup, R. S. Langer, G. A. Ameer. Single chain antibody fragment-based adsorbent for the extracorporeal removal of beta(2)-microglobulin, Kidney International 65 (2004) 310-322.
[13] A. Fernandez and J. J. Ramsden. On adsorption-induced denaturation of folded proteins. J. Biol. Phys. Chem. 1 (2001) 81-84.
[14] J.J. Ramsden, G.I. Bachmanova, A.I. Archakov. Immobilization of proteins to lipid bilayers, Biosensors Bioelectronics 11 (1996) 523-528.
[15] V. Davankov, M. Tsyurupa, M. Ilyin, L. Pavlova. Hypercross-linked polystyrene and its potential for liquid chromatography: A mini review, Journal of Chromatography A 965 (2002) 65-73.
[16] S. Durie, K. Jerabek, C. Mason, D. C. Sherrington. One-pot synthesis of branched poly(styrene-divinylbenzene) suspension polymerized resins, Macromolecules 35 (2002) 9665-9672.
[17] D. Horák, F. Lednický, M. Bleha. Effect of inert components on the porous structure of 2-hydroxyethyl methacrylate-ethylene dimethylacrylate copolymers, Polymer 37 (1996) 4243-4249.
[18] K. Jeřábek, L. Hanková. Functional polymers prepared from p-styrenesulfonyl chloride as the functional monomer, Industrial Engineering Chemical Research 34 (1995) 2598-2604.
[19] F. S. Macintyre, D. C. Sherrington. Control of porous morphology in suspension polymerized poly(divinylbenzene) resins using oligomeric porogens, Macromolecules 37 (2004) 7628-7636.
[20] O. Okay. Phase separation in free-radical crosslinking copolymerisation: formation of heterogeneous polymer networks, Polymer 40 (1999) 4117-4129.
[21] O. Okay. Macroporous copolymer networks, Progress in Polymer Science 25 (2000) 711-779.
[22] I. C. Poinescu, C. Beldie, V. Cotan. Styrene-divinylbenzene copolymers: influence of the diluent on network porosity, Journal of Applied Polymer Science 29 (1984) 23-34.
[23] I. C. Poinescu, V. Cotan. Effect of polymeric porogens on the properties of poly(styrene-co-divinylbenzene), European Polymer Journal 33 (1997) 1515-1521.
[24] B. P. Santora, M. R. Gagné, K. G. Moloy, N. S. Radu. Porogen and crosslinking effects on the surface area, pore volume distribution and morphology of macroporous polymers obtained by bulk polymerisation, Macromolecules 34 (2001) 658-661.
[25] D. C. Sherrington. Preparation, Structure and morphology of polymer supports, Chemical Communications 21 (1998) 2275-2286.

[26] F. Svec, M. J. Fréchet. Temperature a simple and efficient tool for the control of pore size distribution in macroporous polymers, Macromolecules 28 (1995) 7580-7582.
[27] M. P. Tsyurupa, V. A. Davankov. Hypercrosslinked polymers: Basic principles of preparing the new class of polymeric materials, Reactive and Functional Polymers 53 (2002) 193-203.
[28] M. P. Tsyurupa, V. A. Davankov. Porous structure of hypercrosslinked polystyrene: State-of-the-art mini-review, Reactive and Functional Polymers 66 (2006) 768-779.
[29] X. X. Zhu, K. Banana, R. Yen. Pore size control in crosslinked polymer resins by reverse micellar imprinting, Macromolecules 30 (1997) 3031-3035.
[30] X. X. Zhu, K. Banana, H. Y. Liu, M. Krause, M. Yang. Cross-linked porous polymer resins with reverse micellar imprints: Factors affecting the porosity of the polymers, Macromolecules 32 (1999) 277-281.
[31] H. G. Barth, B. E. Boyes, C. Jackson. Size exclusion chromatography and related separation techniques. Analytical Chemistry 70 (1998) 251-278.
[32] E. G. Malawer, L. Senak. Introduction to size exclusion chromatography, in: Handbook of size exclusion chromatography and related techniques, C. Wu (Ed.). Second edition, Marcel Dekker, New York, 2004 pp. 1-24.
[33] E. Meehan. Semirigid polymer gels for size exclusion chromatography, in: Handbook of size exclusion chromatography and related techniques, C. Wu (Ed.). Second edition, Marcel Dekker, New York, 2004 p. 25-44.
[34] H. Yoshizawa, M. Maruta, S. Ikeda, Y. Hatate, Y. Kitamura. Preparation and pore-size control of hydrophilic monodispersed polymer microspheres for size-exclusive separation of biomolecules by the SPG membrane emulsification technique, Colloid Polymer Science 282 (2004) 965-971.
[35] U. Hellburg, J. Ivarsson, B. Johansson. Characteristics of superdex preparatory grade media for gel filtration chromatography of proteins and peptides, Process Biochemistry 31 (1996) 163-172.
[36] S. A. Jones, M. Brown, G. P. Martin. Determination of polyvinyl alcohol using gel filtration liquid chromatography, Chromatographia 59 (2004) 43-46.
[37] P. DePhillips, A. M. Lenhoff. Pore size distributions of cation-exchange adsorbents determined by inverse size-exclusion chromatography, Journal of Chromatography A 883 (2000) 39-54.
[38] D. H. Freeman, I. C. Poinescu. Particle porosimitry by inverse gel permeation chromatography, Analytical Chemistry 49 (1977) 1183-1188.

[39] L. Hagel, M. Östberg, T. Andersson. Apparent pore size distributions of chromatography media. Journal of Chromatography A 743 (1996) 33-42.
[40] Y. Yao, A. M. Lenhoff. Determination of pore size distributions of porous chromatographic adsorbents by inverse size-exclusion chromatography, Journal of Chromatography A 1037 (2004) 273-282.
[41] L. Hagel. Pore size distributions, in: Journal of Chromatography Library – Volume 40, Aqueous Size-Exclusion Chromatograhy, P.L. Dubin (Ed.). Elsevier, Netherlands, 1988,. pp. 119-155.
[42] Seaton, N.A., Walton, J.P.R.B., and Quirke, N. A new analysis method for the determination of the pore size distribution of porous carbons from nitrogen adsorption measurements. Carbon, 1989;27(6):853-861
[43] Ramsden, J.J. Dynamics of protein adsorption at the solid/liquid interface. Recent Res. Devel. Phys. Chem. 1997;1:133-142.
[44] Ramsden, J.J. Adsorption kinetics of proteins. In: A. Hubbard, editor. Encyclopaedia of Surface and Colloid Science, New York: Dekker, 2002, p. 240-261.
[45] Ball, V. and Ramsden, J.J. Analysis of hen egg white lysozyme adsorption on $Si(Ti)O_2$-aqueous solution interfaces at low ionic strength: a biphasic reaction related to solution self-association. Colloids Surfaces B. 2000;17:81-94.
[46] Kurrat, R., Prenosil, J.E. and Ramsden, J.J. Kinetics of human and bovine serum albumin adsorption at silica-titania surfaces. J. Colloid Interface Science. 1997;185:1-8.
[47] Suzuki, M. and Kawazoe, K. Batch measurement of adsorption rate in an agitated tank – pore diffusion kinetics with irreversible isotherm. Journal of Chemical Engineering of Japan. 1974; 7:346-350.
[48] Thomas, S.R. Modelling and simulation of the kidney. Journal of Biological Physics and Chemistry. 2005; 5:70-83.

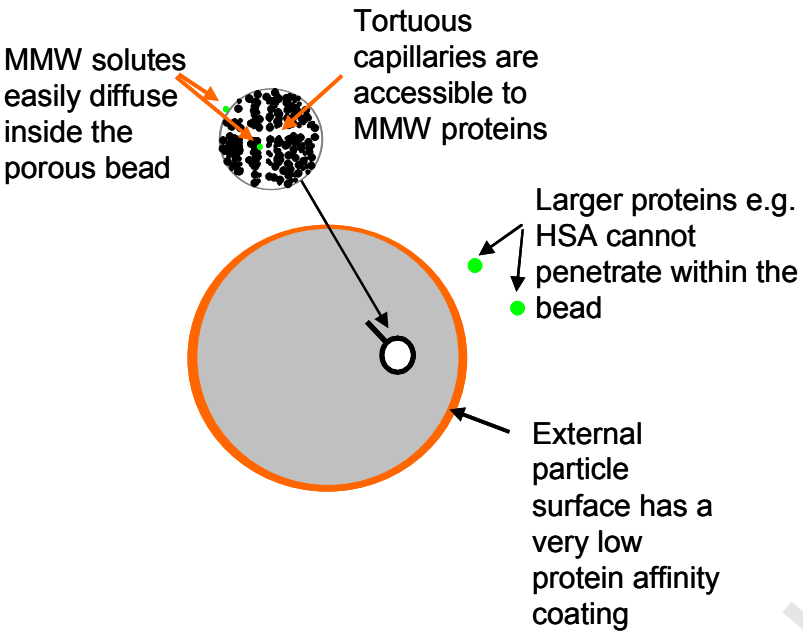

Figure 1. Schematic diagram of a size selective adsorbent bead, with a nanoporous structure suitable for size exclusion of HSA whilst permitting smaller proteins e.g. lysozyme, to diffuse within.

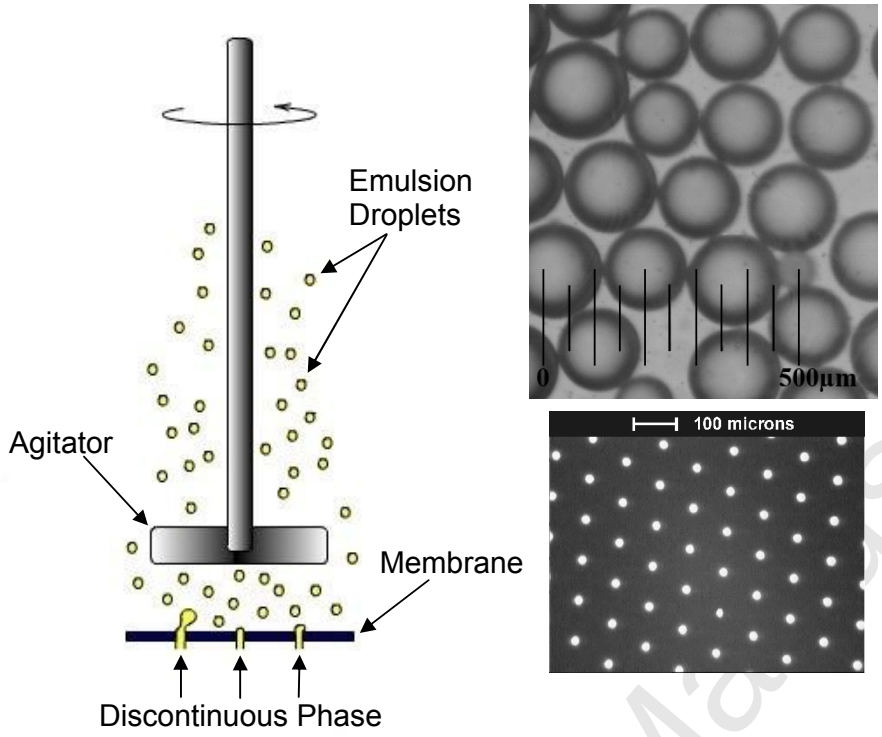

Figure 2. Schematic diagram of emulsion generation in a dispersion cell (left) and micrographs of a circular pore membrane (lower right, courtesy of Micropore Technologies) and a polymer droplet emulsion (size range 130–170 μm) generated using the dispersion cell (upper right).

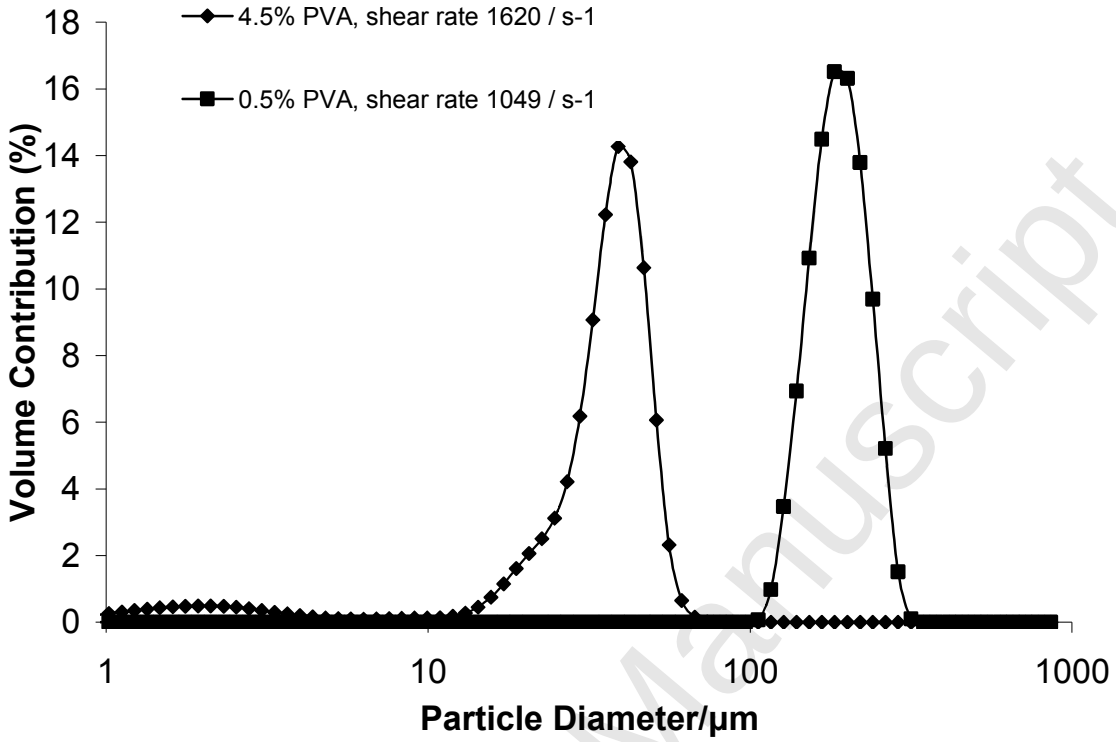

Figure 3. Particle size distributions for polystyrene co-divinylbenzene resins prepared using a 10μm circular pore membrane (Micropore Technologies) but with different PVA concentrations and shear rates. Coefficients of variation (CV) were typically around 20%, compared with 40% for materials prepared using a conventional stirred tank system.

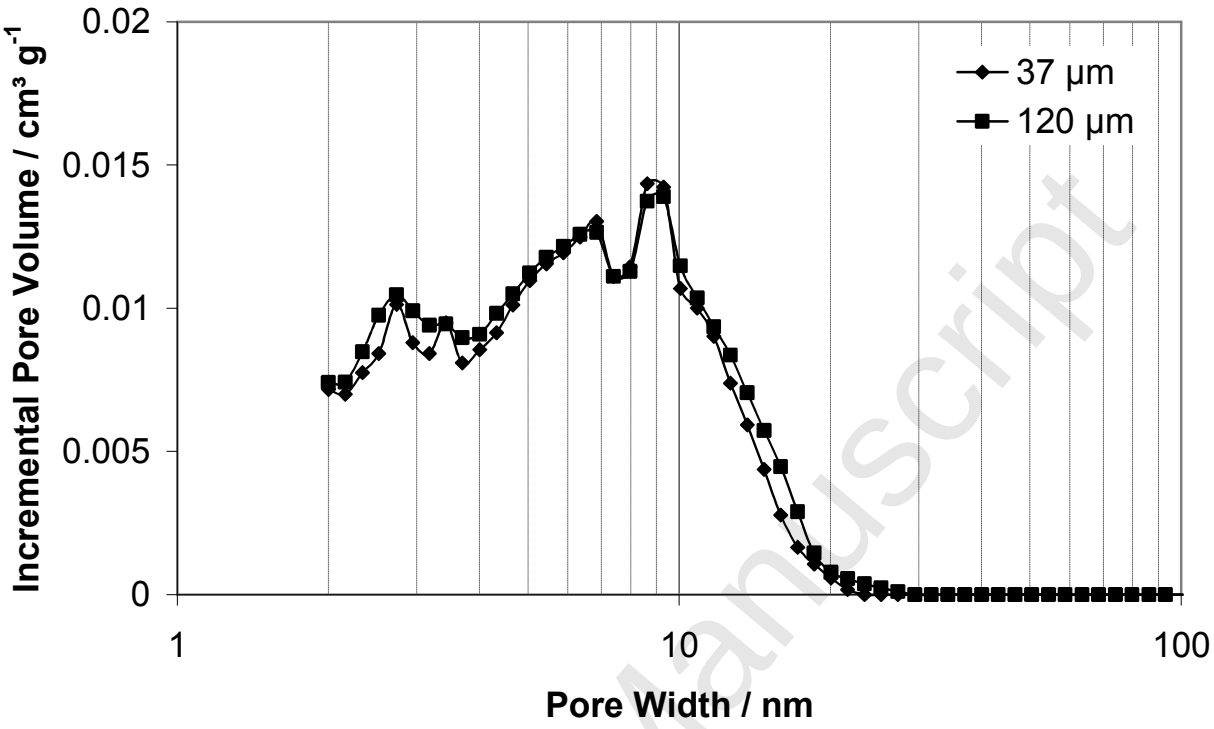

Figure 4. Incremental pore volume distribution for PSDVB3:5TolUn1:0 (prepared as beads of median diameters of 37 and 120 μm).

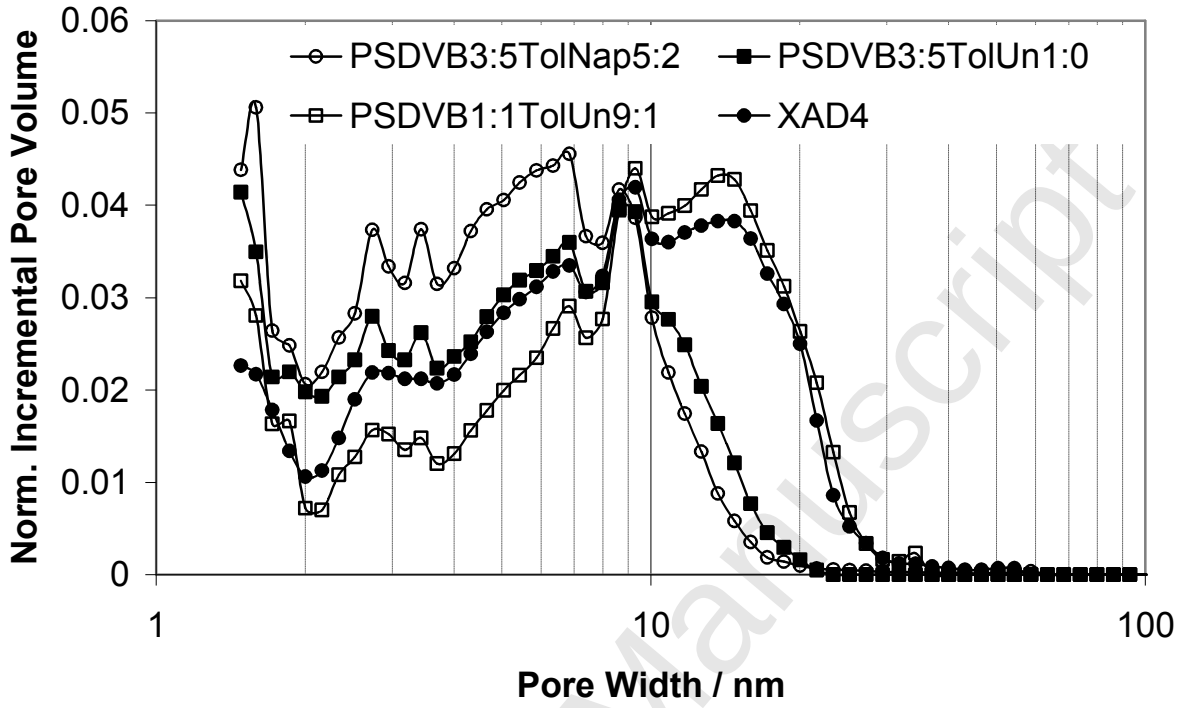

Figure 5. Normalised incremental pore volume distributions resulting from the use of different porogens.

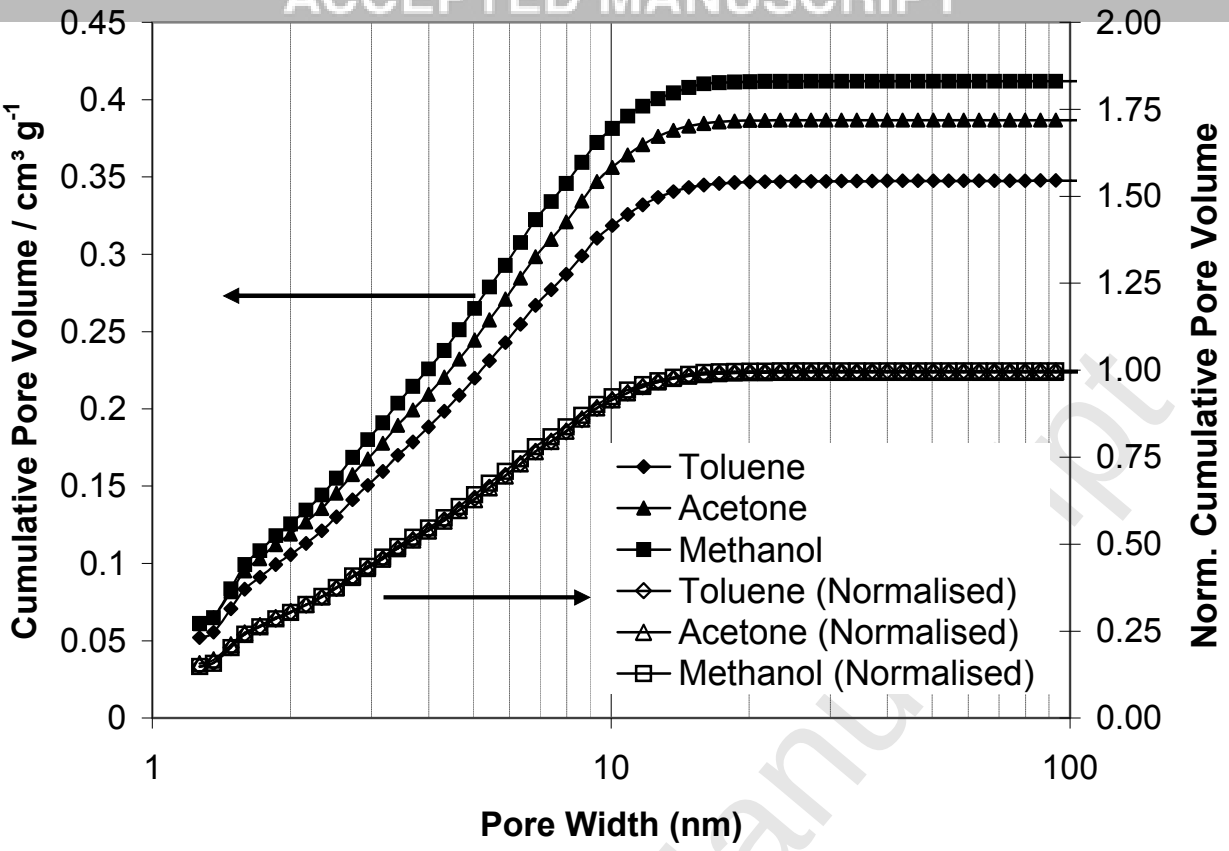

Figure 6. Cumulative and normalized (to the total cumulative volume) cumulative pore volume distributions for PSDVB3:5TolNap5:2 dried from different solvents.

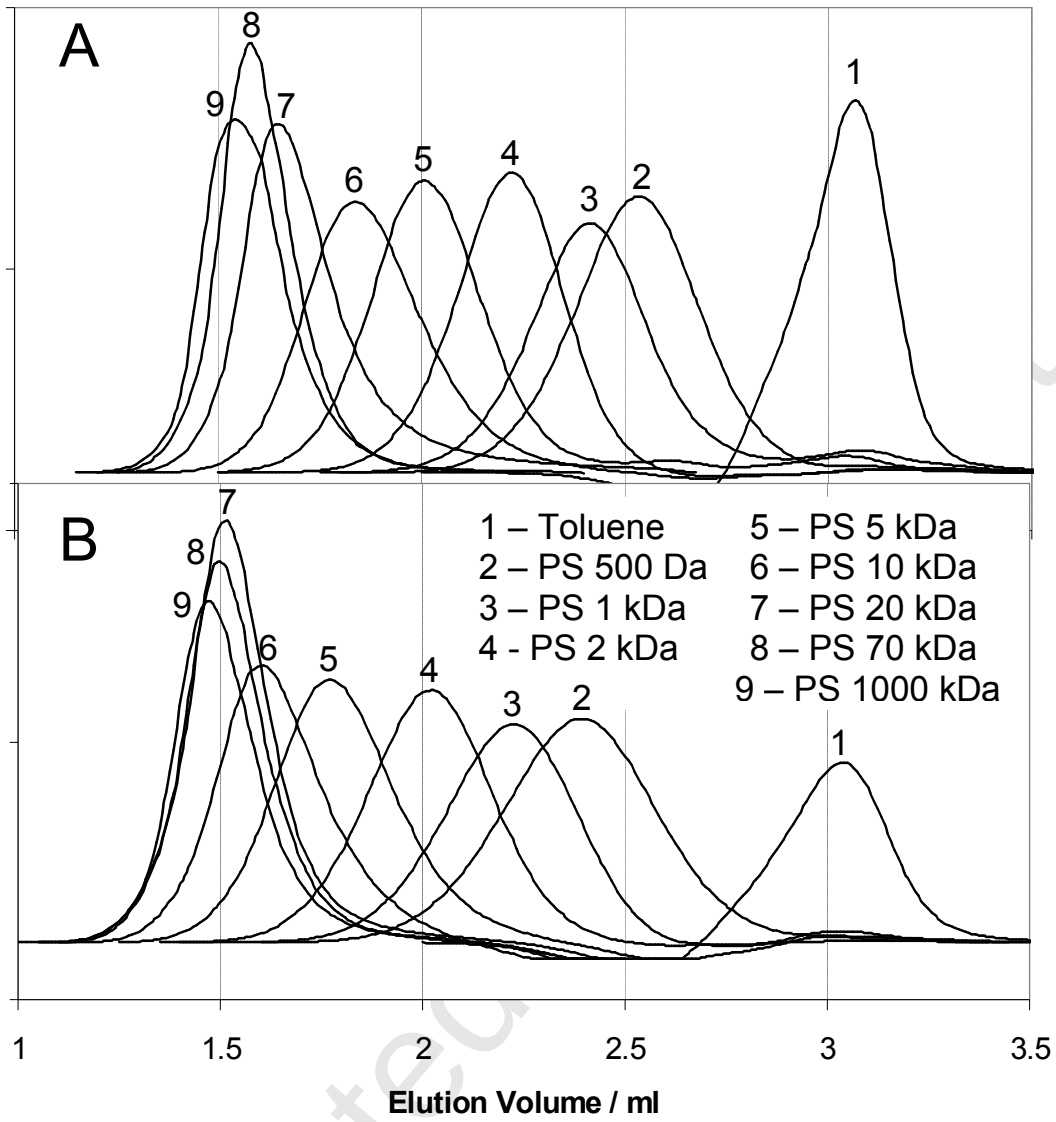

Figure 7. ISEC chromatograms for (A) PSDVB1:1TolUn9:1 and (B) PSDVB3:5TolNap5:2 polymer samples.

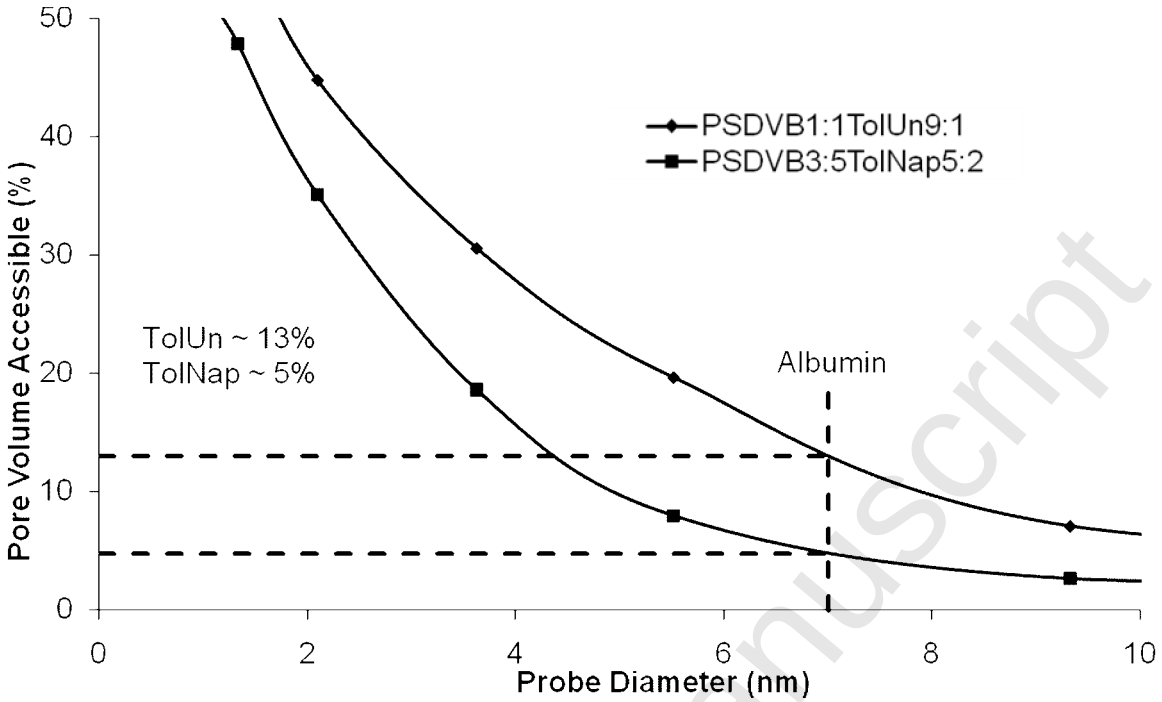

Figure 8. Percentage of pore volume accessible to probes determined from ISEC, comparison of PSDVB1:1TolUn9:1 and PSDVB3:5TolNap5:2 polymer samples (lines connecting the points are merely to guide the eye).

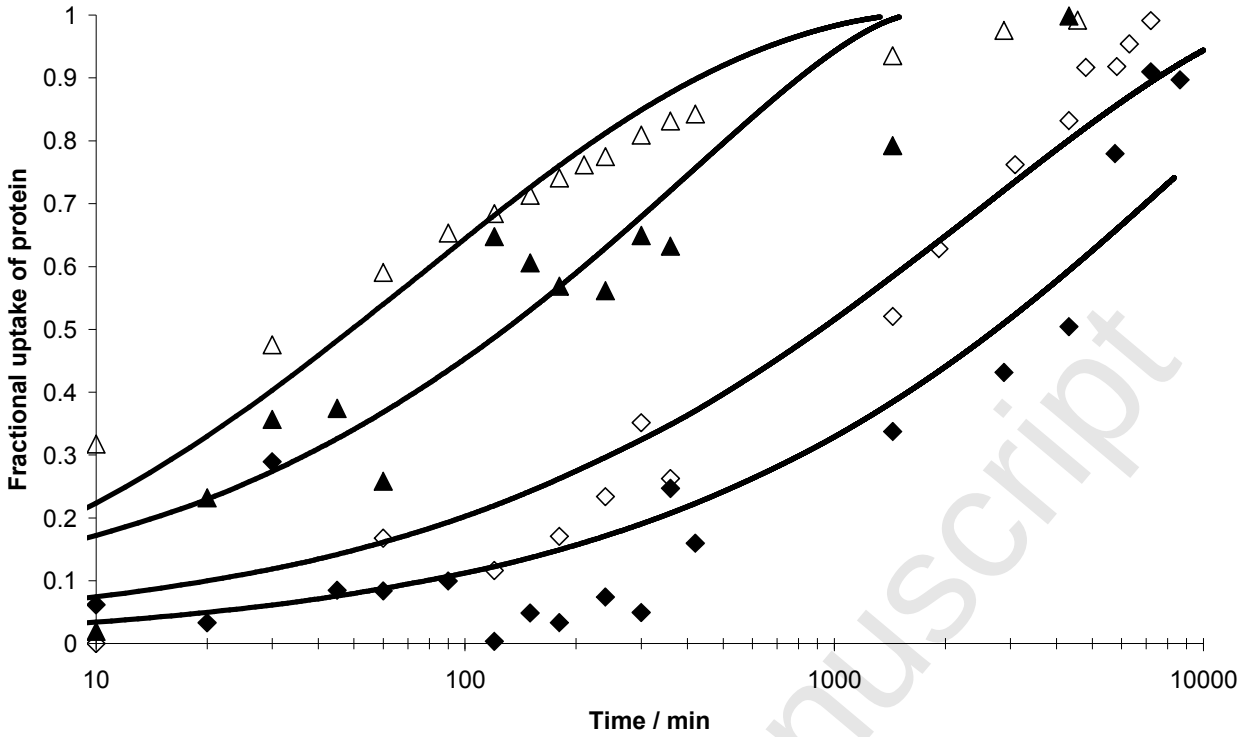

Figure 9. Fractional uptake (q(t)/q*) versus adsorption time, comparison of PSDVB3:5TolNap5:2 polymer sample (open triangles – LYZ data; solid triangles – HSA data) and XAD4 polymer sample (open diamonds – LYZ data; solid diamonds – HSA data). Solid lines are the irreversible isotherm model predictions for the data.

Table 1. Monomer phase compositions for polymer samples, all ratios w/w.

Sample i.d.	Ratio of Styrene to DVB	Nominal Crosslinking %	Porogens		Ratio of Porogens (1:2)
			1	2	
PSDVB3:5TolNap5:2	3:5	50	Toluene	Naphthalene	5:2
PSDVB3:5TolUn1:0	3:5	50	Toluene	-	1:0
PSDVB1:1TolUn9:1	1:1	40	Toluene	Undecane	9:1

Table 2. Polystyrene probe weight average molecular weight (M_P), polydispersity index (PDI) and viscosity radius (R_η).

Probe	M_P / kDa	PDI	R_η / nm[a]
Toluene	0.092	1	-
PS 0.5 kDa	0.374	1.22	0.4
PS 1 kDa	0.89	1.12	0.7
PS 2 kDa	1.92	1.06	1.1
PS 5 kDa	4.87	1.05	1.8
PS 10 kDa	9.95	1.03	2.8
PS 20 kDa	24.3	1.02	4.7
PS 70 kDa	76	1.03	9.1
PS 1000 kDa	1044	1.14	42.6

a - Calculated values [41].

Table 3. Average bead sizes of the adsorbents used in ISEC.

Sample i.d.	Particle Diameter / μm		
	Mean	Median	Mode
PSDVB3:5TolNap5:2	29	28	30
PSDVB1:1TolUn9:1	29	30	36
PSDVB1:1TolUn1:0	34	37	39

Table 4. Surface area and pore volume measurements for polymer adsorbents.

Sample i.d.	BET		DFT			
	Surface Area / $m^2\ g^{-1}$	Pore Volume / $cm^3\ g^{-1}$	Surface Area / $m^2\ g^{-1}$		Pore Volume / $cm^3\ g^{-1}$	
			2 - 10 nm	10 - 50 nm	2 - 10 nm	10 - 50 nm
PSDVB3:5TolNap5:2	412	0.34	88	4	0.18	0.03
PSDVB3:5TolUn1:0	478	0.41	101	9	0.21	0.05
PSDVB1:1TolUn9:1	356	0.47	76	26	0.18	0.19
Amberlite XAD4	830	1.1	222	51	0.5	0.36

Table 5. Lysozyme (LYZ) and Albumin (HSA) total adsorption capacity q* and Γ values for adsorbent materials.

Sample i.d.	LYZ			HSA		
	q* / mg g^{-1}	[a]Γ / mg m^{-2}	Area accessible / m^2 g^{-1}	q* / mg g^{-1}	[b]Γ / mg m^{-2}	Area accessible / m^2 g^{-1}
PSDVB3:5TolNap5:2	59 $\pm$ 7	2.7	22	2.2 $\pm$ 1	2.4	0.9
XAD4	330 $\pm$ 60	2.8	120	95 $\pm$ 5	2.4	40

[a] approximate footprint of lysozyme, 9 nm^2; [b] approximate footprint of albumin, 49 nm^2

Table 6. Summary of experimental variables used for measuring LYZ and HSA batch adsorption dynamics

	TN_5:2	**TN_5:2**	**XAD4**	**XAD4**
Solute	♣LYZ	♠HSA	♣LYZ	♠HSA
Particle size, $d_{3,2}$ x 10^6 (m)	28	197	576	163
Mass of sorbent, (g)	2.5	22	5	0.5
C_o, (mg/l)	402	204	5361	200
C_f, (mg/l)	107	106	2058	105
Saturation uptake, q* (g/g)	0.059	0.0022	0.330	0.095
Stirrer speed, rpm (min^{-1})	726	726	726	726
Porosity, ε (-)	0.29	0.29	0.55	0.55
Solid density, ρ (kg/m^3)	1040	1040	1120	1120
Intraparticle Diffusivity, D_e x 10^{12} (m^2/s)	0.4	40	4	50

♣ Diffusivity in solution ($1x10^{-10}$, m^2/s); ♠ Diffusivity in solution ($6.1x10^{-11}$, m^2/s)